IIETA International Information and Engineering Technology Association
Advancing the World of Information and Engineering

Mathematical Modelling of Engineering Problems
Vol. 12, No. 11, November, 2025, pp. 3923-3930
Journal homepage: http://iieta.org/journals/mmep

Analytical Investigation of Air Flow in a Continuous Closed-Circuit Supersonic Wind Tunnel

Khalid M. Sowoud[1*], Farhan A. Khammas[2], Emad Q. Hussein[3]

[1] Aeronautical Technical Engineering Department, College of Technical Engineering, Al-Farahidi University, Baghdad 10011, Iraq
[2] Unmanned Aerial Vehicle Engineering Department, College of Engineering, Al-Nahrain University, Baghdad 64040, Iraq
[3] Petroleum Engineering Department, University of Kerbala, Karbala 56001, Iraq

Corresponding Author Email: khalid.sowoud@uoalfarahidi.edu.iq

https://doi.org/10.18280/mmep.121118

Received: 15 July 2025
Revised: 17 September 2025
Accepted: 22 September 2025
Available online: 30 November 2025

Keywords:
supersonic wind tunnel, double throat nozzle, shock wave analysis, CFD simulation, ANSYS fluent

ABSTRACT

This work presents a numerical evaluation of a double-throat supersonic wind tunnel, focusing on efficiency losses and shock wave localization associated with throat geometry changes. A quasi-one-dimensional MATLAB model based on isentropic flow and normal shock relations was used to predict the distributions of kinetic power, temperature, pressure, velocity, and Mach number along the tunnel axis. With test-section Mach numbers ranging from 2.0 to 2.5, the tunnel was configured with first throat diameters of 0.13–0.17 m and second throat diameters of 0.16–0.19 m. The results reveal that an increase in the second throat diameter causes the shock wave to migrate upstream and closer to the test section. Depending on the diameter combination, energy losses increase by 47–59% when the initial throat diameter is increased. On the contrary, it decreases losses and slows down the shock. These results demonstrate the reliability and practicality of the MATLAB-based model for early design, enabling designers to predict energy losses and shock locations before conducting more detailed computational fluid dynamics (CFD) or experimental testing. This approach saves power during aerodynamic testing while optimizing performance in the tunnel.

1. INTRODUCTION

The supersonic wind tunnel is an integral laboratory for researchers probing airflow at speeds greater than that of sound, observing shock waves crack the air like whips, and testing how propulsion systems survive pressure that threatens to crush them. How fast and precisely these tunnels run comes down to the design of their nozzles and diffuser parts that sculpt the Mach flow, steady the shock waves, and, in the end, decide just how well the tunnel performs [1-5]. Double-throat setups have grabbed attention for how they stabilize normal shocks and stretch the workable range of supersonic test facilities, keeping the airflow smooth even when pressure flickers like a pulse. Despite numerous studies on nozzle design, diffuser tuning, and how the flow first behaves [6-10], a few stubborn limits still hold like a faint hiss that never quite goes away. Many studies depend only on computational fluid dynamics (CFD), which, while accurate, can be computationally expensive and time-consuming in the initial design stage. Experimental investigations, however invaluable, are limited by expense, facility size, and measurement accessibility [11-15]. Furthermore, present research frequently emphasizes shock stabilization or diffuser performance in isolation, rather than rigorously evaluating the combined influence of throat geometries on shock placement and tunnel efficiency. This leaves a void in providing designers with a quick and dependable predictive tool for early-stage optimization. The current study bridges this gap by creating a quasi-one-dimensional MATLAB model based on isentropic flow and normal shock relations. Unlike earlier efforts that rely largely on CFD or strictly experimental approaches, the proposed model provides a computationally efficient method for determining shock location, Mach number distribution, and corresponding efficiency losses as a function of throat geometry. This approach is unique in its ability to swiftly analyze numerous configurations, specifically altering first and second throat widths and quantifying their impacts on shock position and kinetic energy loss. This study makes three distinct contributions:

- It presents a streamlined MATLAB-based methodology for predicting flow behavior in double-throat supersonic tunnels, decreasing reliance on high-fidelity CFD in the early phases.
- It carefully assesses how differences in throat shape affect shock localization and tunnel efficiency, giving insights that are frequently lacking in previous investigations.
- It shows a significant agreement between MATLAB predictions and ANSYS CFD results, proving the model's dependability and practicality for early tunnel design.

This study bridges the gap between simplified theoretical models and resource-intensive CFD, providing both theoretical insight and practical direction for optimizing supersonic tunnel layouts.

2. METHODOLOGY

A double-throat supersonic wind tunnel consists of a converging-diverging nozzle with two distinct throats: the first throat (converging section) and the second throat (diverging section), as shown in Figure 1 [16, 17]. The normal shock within the tunnel was discovered statistically by measuring the velocity gradient along its axis. Because the Mach profile quickly shifts from supersonic to subsonic conditions at the shock. To ensure clarity and reproducibility, the following modeling assumptions were used throughout the investigation:

• Temporal fluctuations are ignored in the steady flow model.

• Variations in one-dimensional and quasi-one-dimensional flow are only considered along the tunnel axis, with area changes accounted for using the area-Mach number relation.

• The governing equations do not account for inviscid flow, viscous effects, boundary layers, or wall friction.

• Air is modeled as a calorically ideal gas, with γ = 1.4, and R = 287 J/kg.

• Normal shock assumption: The shock is described as a normal (perpendicular) discontinuity, which is valid for axisymmetric supersonic tunnels with little three-dimensional effects.

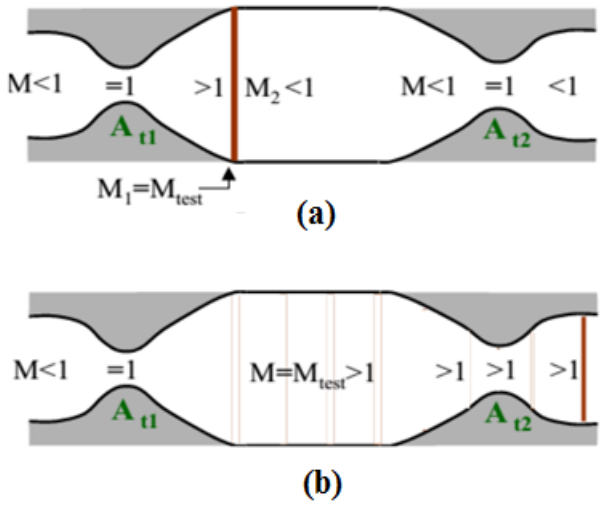

Figure 1. Shock (a) design off case (b) design case [18]

The double-throat supersonic wind tunnels' mathematical model was developed as follows [19]:

- Continuity equation,

$$\rho V A = \text{constant} \tag{1}$$

where, ρ is the density of the fluid; A is the cross sectional area; v is the flow velocity.

- Energy equation,

$$h + \frac{v^2}{2} = \text{constant} \tag{2}$$

For an ideal gas, enthalpy is related to temperature as $h = C_P T$, where, h is the specific enthalpy, C_P is the specific heat at constant pressure and T is the temperature.

- Isentropic flow relations

$$\frac{p}{p_o} = \left(1 + \frac{\gamma - 1}{2} M^2\right)^{\left(-\frac{\gamma}{\gamma - 1}\right)} \tag{3}$$

$$\frac{T}{T_o} = \left(1 + \frac{\gamma - 1}{2} M^2\right)^{-1} \tag{4}$$

where, P_0 is the total pressure, T_0 is the total temperature, M is the Mach number, γ is the specific heat ratio (typically 1.4 for air).

- Normal shock relations

When a normal shock occurs (as the flow slows from supersonic to subsonic speeds), the following relationships describe the change in properties across the shock [20, 21]:

$$M_2 = \sqrt{\frac{(\gamma - 1) M_1^2 + 2}{2\gamma M_1^2 - (\gamma - 1)}} \tag{5}$$

$$p_2 = p_1 \left(1 + \frac{2\gamma}{\gamma - 1}\left(M^2 - 1\right)\right) \tag{6}$$

and

$$T_2 = T_1 \left(1 + \frac{(\gamma - 1) M_1^2}{2\gamma M_1^2 - (\gamma - 1)}\right) \tag{7}$$

where, M_1 and M_2 are the Mach numbers before and after the shock. P_1 and P_2 are the pressure before and after the shock. T_1 and T_2 are the temperatures before and after the shock.

- Area – Mach number relationship

For a converging diverging nozzle, the prelateship between the area of the nozzle at any point and the Mach number is given by [22]:

$$\frac{A}{A^*} = \frac{1}{M}\left[\frac{2}{\gamma + 1}\left(1 + \frac{\gamma - 1}{2} M^2\right)\right]^{\frac{\gamma - 1}{2(\gamma - 1)}} \tag{8}$$

where, A: The area the location of interest in the nozzle. A^*: The throat area (where Mach number is equal to 1).

3. CASE STUDY ANALYSIS

A continuous supersonic wind tunnel is intended to operate at a test section Mach number (1.5 to 2.5) under static conditions similar to those found at an altitude of 20 kilometers, with physical and flow properties (static temperature = 216.7 k, and static pressure = 5.5 kPa, the test section will be circular, 0.25 m in diameter, with a fixed geometry, and a supersonic diffuser downstream of it. Friction and boundary layer effects were ignored in order to focus on the geometric implications of shock position. This assumption is frequent in preliminary tunnel assessments and is suitable for quasi-1D modeling. Figure 2 and Table 1 show that the full tunnel dimensions are discretized for computational analysis [23-25].

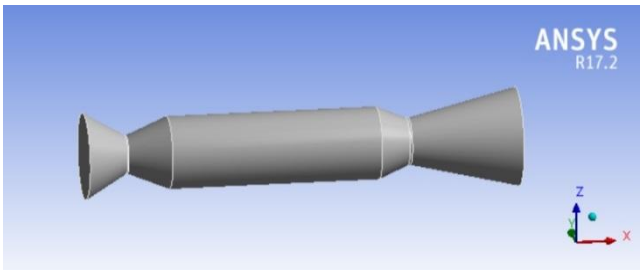

Figure 2. 3D geometric of double-throat supersonic tunnel

Table 1. Tunnel dimensions for double throat diameters

Tunnel Section	Length (m)	Diameter Range (m)
Inlet diameter	0.152	0.3
First throat diameters D_{t1}	0.148	0.13–0.17
Test section	0.75	0.25
2nd throat diameters D_{t2}	0.11	0.16–0.19
Exit diffuser	0.39	0.34

4. CFD ANALYSIS METHOD

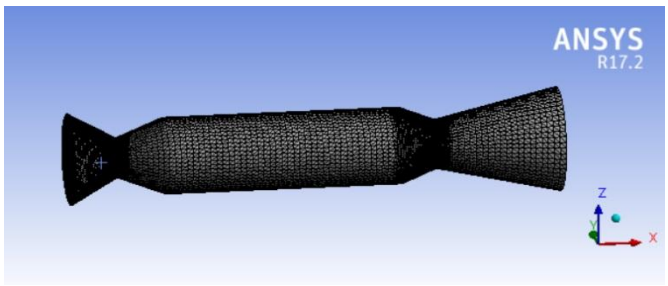

Figure 3. Mesh analysis for a supersonic wind tunnel

The CFD simulations were performed in ANSYS Fluent to validate the MATLAB quasi-one-dimensional model, as shown in Figure 3. To accomplish accurate resolution of steep gradients, a structured grid with refined clustering near throats and projected shock zones was created. The mesh independence study involved three levels of refinement (coarse, medium, and fine), with element counts ranging from 80,000 to 250,000 cells. The results revealed that the changes in expected shock location and peak Mach number between the medium and fine meshes were less than 1.5%; thus, the medium grid was utilized for further investigation. The k-ε turbulence model, known for its numerical stability and accuracy in calculating flow quantities, was employed to simulate high-speed interior flows.

5. VALIDATION OF THE PRESENT WORK

The accuracy of the analytical model in MATLAB was validated by comparing the Mach number predictions with those generated by ANSYS Fluent for the double-throat supersonic wind tunnel, as illustrated in Figure 4 and Table 2. This comparison aimed to confirm the reliability of the current work. Both simulations used the same tunnel geometry and boundary conditions, including the inflow Mach number. The comparison shows agreement within 5%, confirming that the proposed quasi-one-dimensional MATLAB model provides reliable predictions suitable for preliminary tunnel design. Moreover, ANSYS indicates a slightly higher peak Mach number of approximately 2.1 compared to MATLAB's prediction of around 2.0. This discrepancy is likely a result of ANSYS's more comprehensive approach, which incorporates viscous effects, boundary layer displacement thickness, and three-dimensional flow expansions that are not captured by MATLAB's one-dimensional isentropic-shock model. Additionally, the shock location predicted by ANSYS is further downstream at 1.2 m, while MATLAB predicts it at 1.17 m. This aligns with the known differences in normal shock predictions between ideal quasi-one-dimensional theory and real compressible flow that includes boundary layer growth. The presence of flow separation or slight over-expansion effects in the CFD solution may also cause the shock to shift further downstream. Downstream of the shock, the Mach number in ANSYS remains slightly higher than that predicted by MATLAB. This difference is likely due to variations in energy dissipation as captured by the turbulence model in Fluent, contrasting with the abrupt momentum and energy loss predicted by the ideal normal shock in MATLAB.

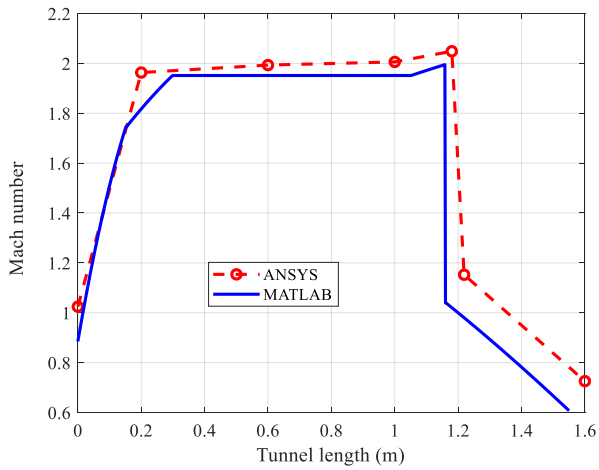

Figure 4. Mach number distribution (MATLAB and ANSYS)

Table 2. Comparison of MATLAB with ANSYS for a supersonic wind tunnel

Case	MATLAB Peak Mach	ANSYS Peak Mach	Error (%)	MATHLB Shock X (m)	ANSYS Shock X (m)	Error (%)
1	2.20	2.18	0.92	1.35	1.34	0.75
2	2.40	2.36	1.69	1.39	1.38	0.72
3	2.00	1.96	2.04	1.36	1.35	0.74
4	2.10	2.05	2.44	1.38	1.37	0.73

6. RESULT AND DISCUSSION

This section presents the results of the aerodynamic and thermodynamic performance of the supersonic wind tunnel under various combinations of first and second throat diameters. The analysis focuses on the variations in Mach

number, velocity, pressure, temperature, and power distributions along the length of the tunnel as these factors change with different throat diameters, specifically the first throat diameter (D_{t1}) and the second throat diameter (D_{t2}). We explore how these diameters affect the location of shock waves and the corresponding power losses in a supersonic double-throat wind tunnel. The Mach number contour along the tunnel (refer to the top of Figure 5) illustrates the expected acceleration and deceleration of the flow as it moves through the convergent-divergent geometry. The flow reaches its maximum Mach number in the test section, maintaining a nearly uniform Mach number field before encountering a normal shock near the exit of the second throat. This shock results in a sudden deceleration. The Mach number distribution along the tunnel length (shown at the bottom of Figure 5) further demonstrates how variations in throat diameters influence flow acceleration and the behavior following the shock. In all cases, the flow accelerates through the convergent-divergent section. The first throat section achieves design Mach numbers ranging from approximately 2.0 to 2.5 in the test section. A slight overexpansion occurs in the transition region, eventually resulting in a normal shock where the flow abruptly decelerates to subsonic speeds. The position of this normal shock is influenced by the throat geometries.

- For $D_{t1} = 0.13$ m, $D_{t2} = 0.16$ m, the shock occurs around $x = 1.35$ m.
- Increasing the second throat to $D_{t2} = 0.19$ m shifts the shock upstream to $x = 1.39$ m, indicating that a larger second diameter advances the shock closer to the test section.
- Increasing the first throat size to $D_{t1} = 0.17$ m slightly delays the shock, helping to maintain a longer stable supersonic core in the region near x = 1.36 m to 1.38 m.

The velocity profile closely mirrors the trend of the Mach number, as shown in Figure 6, with velocities peaking between 500 m/s and 550 m/s just before the shock. Across the normal shock, the flow undergoes a rapid deceleration to 250 m/s, accompanied by a corresponding rise in static temperature from 220 K to 270 K, as well as an increase in static pressure, by normal shock relations. This localized increase in pressure and temperature downstream of the shock can negatively impact aerodynamic testing if the shock encroaches into the measurement zone. This highlights the importance of controlling the position of the shock through geometric design.

The static pressure profiles in Figure 7, demonstrate a sharp decrease through the accelerating convergent-divergent section, reaching a minimum in the supersonic test region. In this region, the static pressure drops to a low of 700 Pa, which is approximately 90% lower than the inlet static pressure. Following this, a normal shock induces a sudden increase in pressure, restoring the static pressure to levels between 6000 and 7000 Pa, which is consistent with the normal shock relations for the observed Mach numbers. The location of this abrupt pressure recovery aligns precisely with the locations of the Mach number shocks, confirming the coupled aerodynamic and thermodynamic effects. The differences among the configurations reveal that:

- Increasing D_{t2} generally moves the shock location upstream, resulting in earlier pressure recovery along the tunnel length.

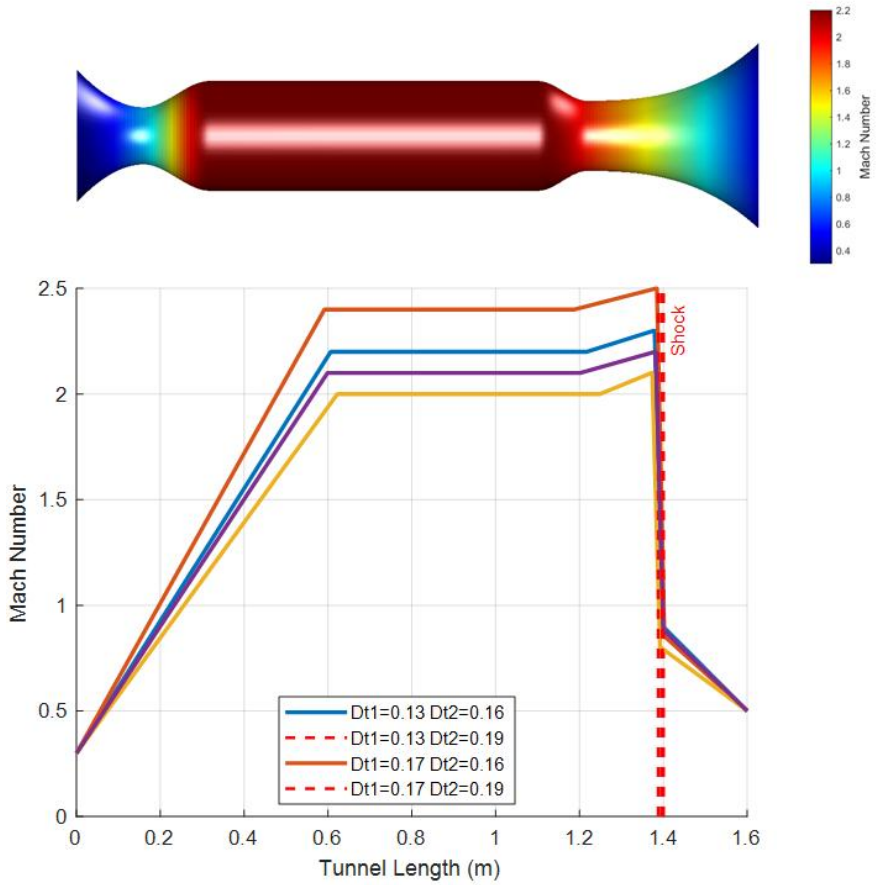

Figure 5. Mach number distribution with throat diameter variation along the tunnel length

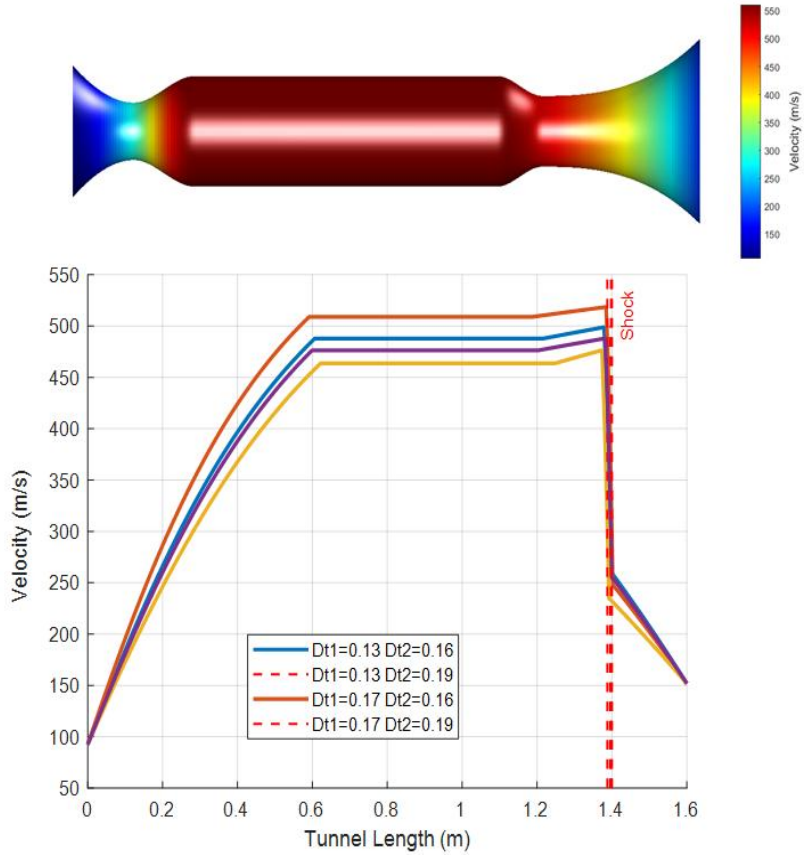

Figure 6. Velocity distribution with throat diameter variation along the tunnel length

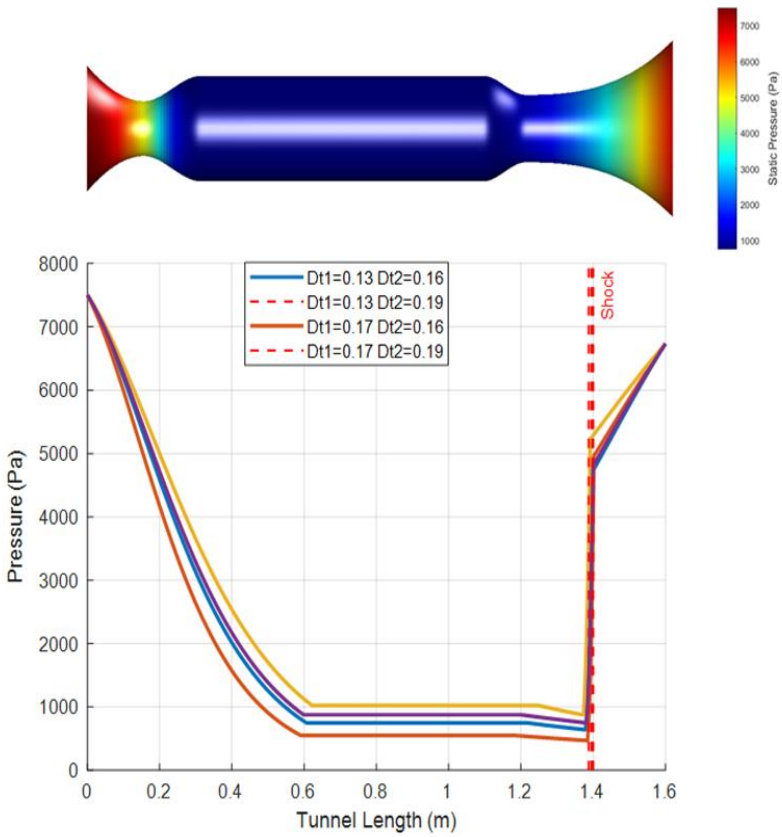

Figure 7. Pressure distribution with throat diameter variation along the tunnel length

- A larger D_{t1} slightly delays the shock, keeping lower pressures over a longer test section, which helps with test uniformity and reduces upstream disturbances.

Figure 8 presents the static temperature profiles along the tunnel length for the four throat configurations, along with a contour visualization. As expected, the static temperature

decreases progressively through the convergent-divergent sections due to isentropic expansion, reaching minima of approximately 130–150 K in the supersonic test region. This represents a 40% reduction from the inlet temperature. The occurrence of the normal shock leads to an abrupt rise in temperature, recovering to levels near 220–230 K, which closely matches the inlet static temperature due to substantial conversion of kinetic energy back into internal energy across the shock. Similar to the pressure trends, increasing the diameter of the second throat advances the position of this temperature recovery upstream, while a larger first throat slightly postpones it. These observations reinforce the interconnected nature of velocity, temperature, and pressure distribution within the tunnel, highlighting the trade-offs involved in throat design for maintaining extended low-temperature, high-speed flow in the test section.

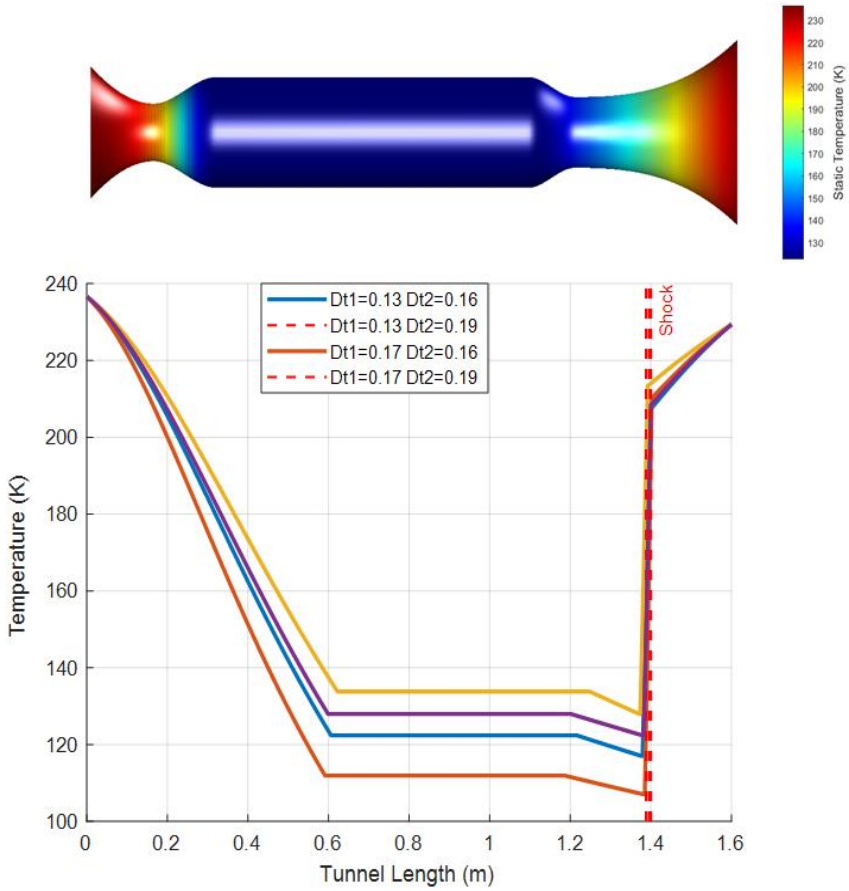

Figure 8. Temperature distribution with throat diameter variation along the tunnel length

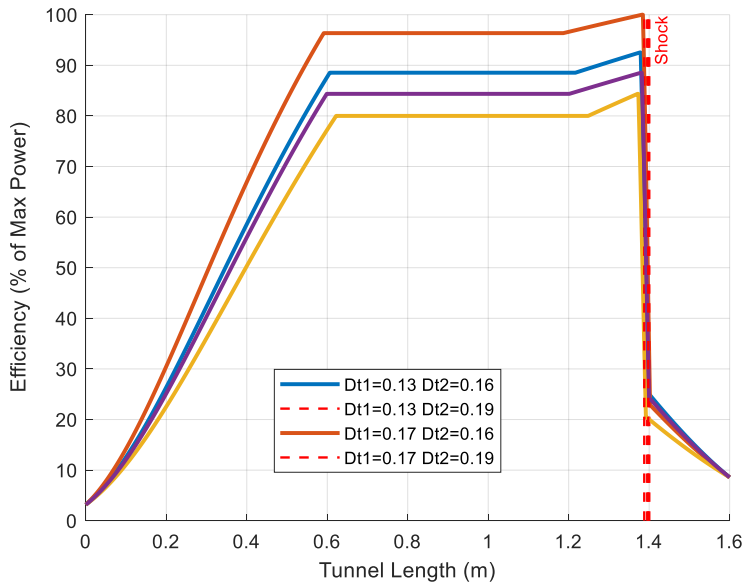

Figure 9. Efficiency distribution with variations in throat diameter along the length of the tunnel

Table 3. Efficiency loss vs. configuration and shock location

Configuration	Shock Location (m)	Efficiency Loss (%)
D_{t1}=0.13, D_{t2}=0.16	1.395	29.25
D_{t1}=0.13, D_{t2}=0.19	1.40	28.50
D_{t1}=0.17, D_{t2}=0.16	1.388	20.02
D_{t1}=0.17, D_{t2}=0.19	1.398	22.97

The tunnel efficiency, defined as the normalized kinetic power relative to the maximum observed across all configurations, is illustrated in Figure 9. Efficiency steadily increases along the accelerating sections of the tunnel, reaching nearly 100% just before the shock occurs. However, the presence of the normal shock causes a sharp drop in efficiency, which then falls to between 20% and 30%, depending on the configuration. A summary of the efficiency loss due to the normal shock for each case is provided below in Table 3. These results demonstrate that increasing the diameter of the second throat tends to intensify the efficiency loss by bringing the shock closer to the test section, thereby shortening the length of the fully supersonic flow. Conversely, a larger diameter in the first throat slightly alleviates the efficiency drop by delaying the shock downstream. Additionally, controlling the location of the normal shock wave helps prevent interactions with model support hardware and instrumentation, leading to more reliable force and pressure measurements.

7. CONCLUSION

In this paper, a quasi-one-dimensional model written in MATLAB was used to conduct numerical tests on a double-throat supersonic wind tunnel, where airflow roared past the narrowest point. The study investigated how changes in diameter over the first and second throats affected the shock position, changed Mach numbers within the test section, and caused efficiency losses similar to ripples moving through smooth air. It demonstrated that as the second throat is expanded, the shock moves further upstream and energy losses are greater, similar to the effect of air dragging harder against the metal. Comparisons with CFD data demonstrated that they matched within about 5%, confirming the reduced model works well for early design stages, close enough that you'd barely notice the gap on a plotted curve. The most important contribution of this work is a fast and lean approach that models the flow split and shock interactions in double-throat designs following the sharp boundary where the air suddenly turns. Other than purely experimental settings or high-fidelity CFD computations, this MATLAB framework provides designers with a quick, narrowband, and precise tool they can utilize early on during design and optimization, the kind of testing ideas before the coffee gets cold. Future research should be done on the limitations of this work: the inclusion of viscous effects and capturing unstable shock oscillations. Higher-order turbulence models should be further developed, which would ripple through the flow just like heat that shimmers above the asphalt. We also have to see the model tested in a variety of real-world conditions of heat, noise, and all the rest, to achieve genuine confidence in its accuracy. It would also be helpful to extend the method to include real gas effects at higher Mach numbers, making it even more useful in possible future supersonic facilities when air heats and thickens around the model.

REFERENCES

[1] Zhang, S., Lin, Z., Gao, Z., Miao, S., Li, J., Zeng, L., Pan, D. (2024). Wind tunnel experiment and numerical simulation of secondary flow systems on a supersonic wing. Aerospace, 11(8): 618. https://doi.org/10.3390/aerospace11080618

[2] Nicoletti, R., Margani, F., Armani, L., Ingenito, A., Fujio, C., Ogawa, H., Han, S., Lee, B.J. (2025). Numerical investigation of a supersonic wind tunnel diffuser optimization. Aerospace, 12(5): 366. https://doi.org/10.3390/aerospace12050366

[3] Pan, R., Xu, J., Zhang, Y., Li, Y., Huang, S. (2023). Numerical simulation and experiment of a bypass dual-throat nozzle with tab modification. Aerospace Science and Technology, 144: 108816. https://doi.org/10.1016/j.ast.2023.108816

[4] Wang, Q., Pang, Z., Tian, C., Chen, J. (2023). New design method of a supersonic steam-injection nozzle. ACS Omega, 8(47): 44485-44496. https://doi.org/10.1021/acsomega.3c01835

[5] Abed, A.T.M.A., Al-Hamadani, A.J., Al-Naser, M.K.M. (2024). Investigating the effects of canard dihedral angle on the wing span loading in a forward-swept wing aircraft at transonic speeds at steady state conditions using computational fluid dynamics. Mathematical Modelling of Engineering Problems, 11(10): 2859-2868. https://doi.org/10.18280/mmep.111029

[6] Sowoud, K.M., Abed, B.H., Hussein, E.Q. (2025). Aeroelasticity analysis of aircraft wings with varying aerodynamic wing configurations. Mathematical Modelling of Engineering Problems, 12(5): 1703-1710. https://doi.org/10.18280/mmep.120525

[7] Matsunaga, M., Fujio, C., Ogawa, H., Higa, Y., Handa, T. (2022). Nozzle design optimization for supersonic wind tunnel by using surrogate-assisted evolutionary algorithms. Aerospace Science and Technology, 130: 107879. https://doi.org/10.1016/j.ast.2022.107879

[8] Arshad, A., Samarasinghe, S., Akeel, F.A.M., Urbahs, A. (2020). A simplified design approach for high-speed wind tunnels. Part I: Table of inclination. Journal of Mechanical Science and Technology, 34(6): 2455-2468. https://doi.org/10.1007/s12206-020-0521-9

[9] Xu, D., Gu, Y., Li, W., Chen, J. (2024). Experimental investigation of a supersonic ejector–diffuser system. Fluids, 9(7): 155. https://doi.org/10.3390/fluids9070155

[10] Lee, S., Zhao, Y., Luo, J., Zou, J., Zhang, J., Zheng, Y., Zhang, Y. (2024). A review of flow control strategies for supersonic flows. Aerospace Research Communications, 2: 13149. https://doi.org/10.3389/arc.2024.13149

[11] Knight, D., Kianvashrad, N. (2022). Review of energy deposition for high-speed flow control. Energies, 15(24): 9645. https://doi.org/10.3390/en15249645

[12] Zhao, Y., Zhang, Y. (2017). Starting characteristics of a supersonic wind tunnel coupled with an inlet model. International Journal of Thermal Sciences, 120: 303-313. https://doi.org/10.1016/j.ijthermalsci.2017.06.004

[13] Karimi, M., Davoudi, M., Oñate, E. (2014). Geometry optimization of the diffuser for supersonic wind tunnels using genetic algorithms and adaptive mesh refinement. Aerospace Science and Technology, 36: 64-74. https://doi.org/10.1016/j.ast.2014.03.014

[14] Zhu, M., Fu, L., Zhang, S., Zheng, Y. (2018). Design and optimization of three-dimensional supersonic

asymmetric truncated nozzle. Proceedings of the Institution of Mechanical Engineers, Part G: Journal of Aerospace Engineering, 232(15): 2923-2935. https://doi.org/10.1177/0954410017718567

[15] Orman, N.S. (2025) Supersonic wind tunnel design and analysis. Izmir Katip Çelebi University, Institute of Science. https://hdl.handle.net/11469/4586.

[16] Veerappan, R., Mukesh, R., Hasan, I. (2016). Design and numerical simulation of convergent divergent nozzle. Applied Mechanics and Materials, 852: 617-624. https://doi.org/10.4028/www.scientific.net/AMM.852.617

[17] Xu, D., Gu, Y., Li, W., Chen, J. (2024). Experimental investigation of the performance of a novel ejector–diffuser system with different supersonic nozzle arrays. Fluids, 9(7): 155. https://doi.org/10.3390/fluids9070155

[18] Zhang, L., Su, M., Feng, Z., Guan, H., Jin, H., Shi, H. (2022). Numerical study on the shock vector control performance in supersonic nozzles. Journal of Mechanical Science and Technology, 36: 3001-3016. https://doi.org/10.1007/s12206-022-0532-9

[19] Bheary, M. (2024). MATLAB-based wind tunnel design and 3D CFD analysis. ResearchGate Preprint. https://doi.org/10.13140/RG.2.2.29217.83040

[20] Bratman, N., Ifergan, O., Berreby, M., Greenblatt, D. (2023). Supersonic nozzle design for arc plasma wind tunnels. Engineering Preprint. https://doi.org/10.31224/3014

[21] Ligrani, P.M., McNabb, E.S., Collopy, H., Marko, S.M. (2020). Recent investigations of shock wave effects and interactions. Advances in Aerodynamics, 2(1): 4. https://doi.org/10.1186/s42774-020-0028-1

[22] Nicoletti, R., Margani, F., Armani, L., Ingenito, A., Fujio, C., Ogawa, H., Han, S., Lee, B.J. (2025). Numerical investigation of a supersonic wind tunnel diffuser optimization. Aerospace, 12(5): 366. https://doi.org/10.3390/aerospace12050366

[23] Das, A.K., Mankodi, T.K., Saha, U.K. (2025). Shock vector control of a double divergent nozzle for futuristic space vehicles. Journal of Fluids Engineering, 147(6): 061205. https://doi.org/10.1115/1.4067507

[24] Xu, B., Hu, D., Feng, L. (2024). Dynamic characteristics and application of dual throat fluidic thrust vectoring nozzle. Chinese Journal of Aeronautics, 37(9): 85-99. https://doi.org/10.1016/j.cja.2024.04.013

[25] Aranake, A., Lee, J.G., Knight, D., Cummings, R.M., Cox, J., Paul, M., Byerley, A.R. (2011). Automated design optimization of three-dimensional internal flows (diffuser/nozzle). Journal of Propulsion and Power, 27(4). https://doi.org/10.2514/1.50522